

THE EFFECT OF δ_3 ON A YAWING HAWT BLADE AND ON YAW DYNAMICS*

Frederick W. Perkins and Robert Jones

Kaman Aerospace Corporation
Old Windsor Road
Bloomfield, Connecticut 06002

ABSTRACT

A single degree of freedom aeroelastic computer model, WMSTAB3, has been employed to perform a parametric analysis of HAWT blade behavior during yaw maneuvers. Over 1,000 different combinations of δ_3 and normal frequency were analyzed.

The effect of δ_3 and flapping stiffness on flapping frequency, phase, and magnitude are discussed. The moments transmitted to the fixed system during yaw maneuvers are calculated and reduced to time constants of response to step changes in wind direction. The significance of the time constants for the configurations considered relative to yaw response rate and lag angle is discussed, along with their possible significance for large HAWT.

INTRODUCTION

The δ_3 hinge is a device which mechanically couples rotor blade pitching and flapping. The δ_3 hinge is typically employed to stabilize lifting rotors by increasing the flapping stiffness and reducing flapping. The stiffness increase also increases the flapping frequency, thereby allowing flexibility in blade tuning to avoid possible structural resonances.

Negative δ_3 is destabilizing. The effect of negative δ_3 is to reduce the flapping frequency, by virtue of reduction in flapping stiffness. The reduction in flapping frequency will be accompanied by increasing flapping as long as the flapping frequency is approaching 1.0 per rev. The phase of flapping response to yaw direction and rate excitations also changes with adjustment of frequency.

These qualitative observations of the effect of δ_3 on the magnitude and phase of flapping response to yaw inputs suggested a quantitative analysis to determine optimum operating configurations for spring restrained teetering type wind turbines. (The δ_3 hinge is easily incorporated in such a rotor by canting the teeter axis and the normal to the feathering axis, as in Figure 1.) Because of the large range of flapping frequencies and candidate δ_3 angles considered, a simple aeroelastic model, WMSTAB3, was developed which could be rapidly executed, yet which retained sufficient sophistication to be acceptable. More than 1,000 possible operating configurations were ultimately analyzed to develop the data reported herein.

The analysis indicates that it is possible to optimize rotor flapping with respect to magnitude

or phase, or yaw performance, quantified by response time and/or restoring or damping moments. The operating conditions required for optimization are often contradictory. For example, it is possible to eliminate flapping in the direction of the tower due to either yaw position or rate excitations, but not both simultaneously.

ANALYTIC BACKGROUND

The equations of motion were derived from fundamental mechanics and a linear aerodynamic representation of the forcing function, paralleling Stoddard (Reference 1). The equation of motion of the flapping wind turbine blade is

$$I_b \ddot{\beta} + \Omega^2 I_b \left(K + \frac{G}{\Omega^2} \phi \psi \right) \beta = \frac{I_b \gamma \Omega^2}{2} \left[\frac{1}{3} \left\{ \mu_0 - \lambda_i \right. \right. \\ \left. \left. - \frac{3}{4} \frac{q}{\Omega} \phi \psi - \left(\frac{3}{4} - \frac{e}{R} \right) \frac{\dot{\beta}}{\Omega} - \frac{3}{4} \left[\beta \tan \delta_3 + \frac{\theta_0}{5} \right. \right. \right. \\ \left. \left. \left. - \theta_p \right] \right\} - \bar{U}_0 \phi \psi \left\{ \mu_0 - \lambda_i - \frac{2}{3} \left[\frac{\theta_0}{4} - \theta_p \right] \right\} \right] \\ + 2 I_b q \Omega \phi \psi$$

where

$$K = 1 + \epsilon + \frac{K_\beta}{I_b \Omega^2}$$

$$\epsilon = \frac{M_b e X_g R^2}{I_b}$$

$$G = \frac{M_b X_g g R}{I_b}$$

*The work reported herein was done as part of a Kaman Aerospace Corporation in-house R & D program.

Substituting

$$\beta = \beta_0 + \beta_{1S}\psi + \beta_{1C}\psi^2$$

$$\beta' = \frac{\partial \beta}{\partial \psi} = \frac{\dot{\beta}}{\Omega}$$

$$\beta'' = \frac{\partial^2 \beta}{\partial \psi^2} = \frac{\ddot{\beta}}{\Omega^2}$$

into the equation of motion, neglecting products of β , α_y , \bar{U}_0 and their derivatives, and rewriting the equation of motion in the frequency domain, we have

$$\begin{bmatrix} K + \frac{\gamma}{8} \tan \delta_3 & \frac{6}{2\Omega^2} - \frac{1}{3} \bar{U}_0 \tan \delta_3 & \frac{\sqrt{\bar{U}_0}}{12} \\ \frac{6}{\Omega^2} - \frac{2}{3} \bar{U}_0 \tan \delta_3 & K - 1 + \frac{\gamma}{8} \tan \delta_3 & \frac{\gamma}{8} (1 - \frac{4e}{3R}) \\ \frac{\sqrt{\bar{U}_0}}{6} & -\frac{\gamma}{8} (1 - \frac{4e}{3R}) & K - 1 + \frac{\gamma}{8} \tan \delta_3 \end{bmatrix} \begin{Bmatrix} \beta_0 \\ \beta_{1C} \\ \beta_{1S} \end{Bmatrix} = \begin{Bmatrix} \frac{\gamma}{2} \left[\frac{1}{3} (\mu_0 - \lambda_i) - \frac{1}{4} \left(\frac{e_0}{5} - e_p \right) \right] \\ -\frac{\gamma}{2} \bar{U}_0 \left[\mu_0 - \lambda_i + \frac{e_0}{6} - e_p \right] - 2\bar{q} \\ -\frac{\gamma}{8} \bar{q} \end{Bmatrix}$$

where terms in harmonics of ψ greater than the fundamental are neglected. This system of equations is solved in program WMSTAB.

The use of linear aerodynamics for the forcing function retains the essential features of a real wind turbine blade, including pitch angle, built-in twist, induced velocity, and blade mass, while sacrificing the accuracy of a more comprehensive aerodynamics analysis. Similarly, the single degree of freedom, flapping, retains the essential feature of a more comprehensive aeroelastic code, the mobility of the blade, while minimizing the computational difficulty. Because of the computational ease of the analysis, it is very useful for the reduction of a large number of candidate operating configurations into general trends.

The program WMSTAB uses the structural characteristics of the Kaman 40 kW wind turbine, where applicable, as the baseline. Those variables dependent on rotor size are proportioned for other radii as follows:

$$\begin{aligned} R &\propto R^1 \\ \Omega &\propto R^{-1} \\ \gamma &\propto R^0 \\ e &\propto R^1 \end{aligned}$$

$$M_b \propto R^3$$

$$I_b \propto R^5$$

$$K_b \propto R^5 \text{ (when flapping frequency is constant).}$$

Three rotor radii were analyzed to illustrate characteristics dependent on rotor size. These radii (4.88 m [16 ft]; 9.76 m [32 ft]; and 19.51 m [64 ft]) were taken to be representative of small, intermediate, and large wind turbines, respectively.

The equation of motion does not include an offset between the yaw axis and the rotor. This offset will have both aerodynamic and dynamic consequences, principally arising from three sources.

First, yaw motions impart an out-of-plane velocity component to the blade, given by

$$\underline{V}_y = \underline{q} \times \underline{r}$$

where the underscore denotes vector quantities. For small values of yaw offset, the magnitude of \underline{r} is essentially equal to the blade radius at points where the aerodynamic forces are large. Hence, the effect of yaw offset on blade translations is second order, and is neglected.

Second, for very low normal frequencies, the tilt of the thrust vector will dominate yaw dynamics. For a true teetered rotor, there are no other yaw restoring or damping moments than those given by the product of the in-plane component of rotor thrust and the yaw offset. The magnitude of these moments depends on the exact value of the yaw offset so they cannot be calculated for a general case.

Third, the yaw offset will cause the inertia of the yawing system to be greater than the flapping inertia of the blades alone. The magnitude of the mass transfer effect again depends upon the magnitude of the yaw offset, and cannot be computed in general.

FLAPPING ANALYSIS

Because of the obvious difficulty in referring to both the actual flapping frequency and the stiffness of the flapping spring as some multiple of Ω , as is customary, the term "normal frequency" was coined to refer to the flapping frequency of the blade when $\delta_3 = 0$. Thus, increasing normal frequency refers to increasing spring stiffness, and a given normal frequency blade may have either increasing or decreasing flapping frequency, depending on δ_3 .

Flapping is defined as the amplitude of the harmonic portion of the β deflections. WMSTAB3 includes only first harmonic flapping. It is probable that this harmonic would include the bulk of flapping energy in an actual wind turbine because the cyclic inputs leading to higher harmonic responses are generally lacking.

Figure 2 shows the dependence of flapping frequency on normal frequency, which is determined by the stiffness of the flapping spring, and on

δ_3 which greatly affects the strength of the aerodynamic spring. The range of normal frequencies was defined by practical considerations of rotor blade design. The relationship between decreasing flapping frequency and decreasing δ_3 , and the converse, is apparent. Flapping instabilities are suggested by the rapid decay of flapping frequencies in the neighborhood of large negative δ_3 angles.

Figures 3 and 4 show the dependence of total flapping induced by yaw position and rate, respectively, on normal frequency and δ_3 . A number of trends are evident. First, for $\delta_3 \geq 0$, increasing normal frequency decreases flapping. This is not necessarily so for $\delta_3 < 0$. Second, the total flapping is determined more by the proximity of the flapping frequency to 1.0 P than by normal frequency. In fact, the amount of flapping available to any normal frequency, given suitable δ_3 , is essentially constant. The third item of major interest is that the flapping due to yaw position is independent of rotor size, but the flapping due to yaw rate increases linearly with rotor size for a fixed yaw rate. This is a consequence of the gyroscopic moments acting on the blade, and gives rise to the yaw dynamics effects discussed later.

Figures 5 and 6 present the phase angle of flapping response to yaw position and rate, respectively. Horizontal blade position corresponds to $\pm 90^\circ$. Consequently, flapping which takes place entirely in the horizontal plane has a phase angle of $\pm 90^\circ$. Comparison of Figures 5 and 6 indicates that it is not possible to totally eliminate flapping in the tower direction. Judicious selection of normal frequency and δ_3 can, however, insure that flapping in the direction of the tower will always be small relative to total flapping. Note that these phase angles are independent of rotor size, and depend only on the flapping frequency (and the pitch angles, a second order effect).

Finally, the flapping induced by yaw direction will depend approximately linearly on wind speed, while the yaw rate induced flapping is essentially independent of wind speed.

The data presented in this section may be used to estimate the yaw performance of a true teeter rotor (zero flapping spring) through the phase angles and flapping angles presented. Again, the results will depend on a particular design and are not included in this analysis.

YAWING BEHAVIOR

The yawing behavior of a wind turbine depends on three things: the aerodynamic spring rate, the total damping, and the yawing inertia. The governing equation of motion

$$I_y \ddot{\alpha}_y + C_y \dot{\alpha}_y + K_y \alpha_y = \text{yaw moments}$$

can be solved as discussed in many texts of elementary dynamics. The contribution of this study

is the generation of linearized estimates for C_y and K_y and the solution of the homogeneous equation of motion, after setting $I_y = I_b$, from which time constants of yaw response to step changes in wind direction were calculated.

Figure 7 is an illustration of the aerodynamic spring constant, K_y , determined by imposing a yaw angle of 10° , and normalizing the result to a yaw angle of 1.0 radian. The peak of the spring rate occurs at the 1.0 P flapping frequency for all of the normal frequencies shown. Instability is suggested by the very large spring constants in evidence for high normal frequencies and large negative values of δ_3 . The stabilizing effect of positive δ_3 is also evident by the convergence of spring constants for large positive δ_3 , suggesting that δ_3 has come to dominate flapping dynamics. Note that the yaw spring constant is a linear function of rotor size. The spring rate is approximately linear with wind speed for fixed yaw angle.

The damping constant C_y is plotted in Figure 8.

Much of what has just been described for Figure 7 is also true here. The most notable exceptions are that the damping rate was normalized to 1.0 radian/sec, and the peak damping occurs at δ_3 angles smaller (more negative) than for the corresponding spring rate. The yaw damping rate is independent (to first order) of wind speed.

The spring rates and damping rates are decoupled in this analysis.

The yaw dynamics behavior can be summarized by calculating the time constant of response to a step change in wind (yaw) direction, as discussed above. These data are assembled in Figure 9. Two trends, increasing time constant first with increasing δ_3 , and second, with increasing normal frequency, are immediately obvious. The time constants also increase linearly with rotor size.

The time constant can be interpreted many ways. Also indicated on ordinate axes of Figure 9 are the time required to decay to 50% amplitude, and the time required to decay to 5% amplitude, which numbers are linear transforms of the time constant. Yet another interpretation is that the product of the time constant and the rate of change of wind direction equals the lag angle between the wind direction and the axis of rotation. Because the time constants increase with increasing rotor diameter, the data indicate that the lag angle for large rotors could be quite large, even if the rate of change of wind direction is quite small. Since this lag angle degrades performance, the evaluation of system productivity, particularly for large rotors in a variable wind, should be evaluated with respect to the lag (yaw) angles almost certain to be present.

CONCLUDING REMARKS

The incorporation of significant amounts of δ_3 into a horizontal axis wind turbine blade greatly increases the options available to the designer. The δ_3 hinge may be used to adjust magnitude or phase of the flapping response to either yaw rate or direction, thus controlling the mechanical and aerodynamic coupling with the fixed system degrees of freedom. The effect of δ_3 on flapping frequency can also be exploited to optimize system dynamics.

The reduction of the blade flapping data into yawing spring and damping constants allows the estimation of response time to changes in wind direction. The data indicate that large wind turbines may suffer large lag angles if operated where winds vary in direction. This may be a source of performance degradation previously overlooked.

REFERENCES

1. Stoddard, F. S.: "Structural Dynamics, Stability and Control of High Aspect Ratio Wind Turbines," PhD. Dissertation, Ocean Engineering, University of Massachusetts, Amherst, Massachusetts, February 1979.
2. Den Hartog, J. P.: Mechanical Vibrations, McGraw Hill (New York), Copyright 1947.

NOMENCLATURE

a	lift slope = 5.73/radian
C	chord
C_y	yaw damping rate
ϕ	cosine
e	offset/R
g	gravitational acceleration
I_b	flapping inertia
I_y	yaw inertia
K_b	flapping spring rate
K_y	aerodynamic yaw spring rate
M_b	rotor blade mass
P	division by Ω
q	yaw rate
\bar{q}	q/Ω
R	rotor blade radius
r	distance from yaw axis to a point on the blade
\$	sine
\bar{U}_0	crosswind/ ΩR
V_y	out-of-plane velocity due to yaw rate
X_g	radius to c.g./R

α_y	yaw angle
β	flapping angle
β_0	steady harmonic coefficient
β_{1c}	cosine harmonic coefficient
β_{1s}	sine harmonic coefficient
γ	lock number $\equiv \rho CaR^4/I_b$
δ_3	angle between normal to feathering axis and teeter axis
θ_0	built-in linear twist (total)
θ_p	pitch angle, + implies increasing thrust
λ_i	induced velocity/ ΩR
u_0	wind velocity/ ΩR
ρ	air density
ψ	azimuth angle
Ω	rotational speed

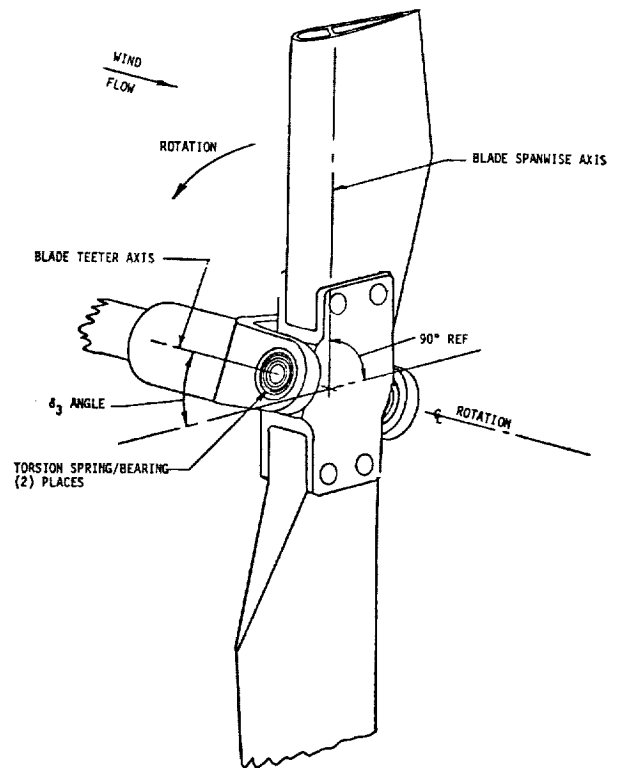


Figure 1 - Teetered rotor showing δ_3 due to offset between teeter axis and the normal to the feather axis.

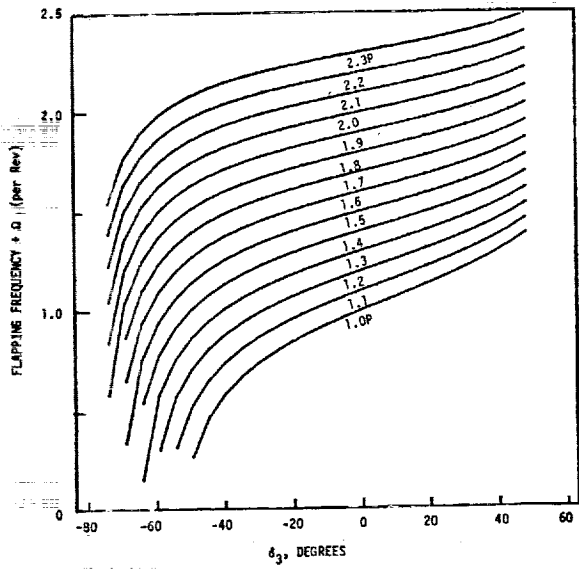


Figure 2 - Flapping frequency vs δ_3 for fourteen normal frequencies.

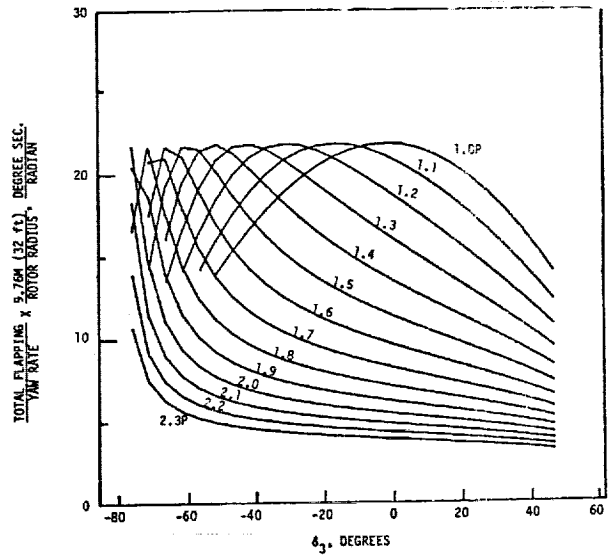


Figure 4 - Total flapping due to yaw rate vs δ_3 for fourteen normal frequencies.

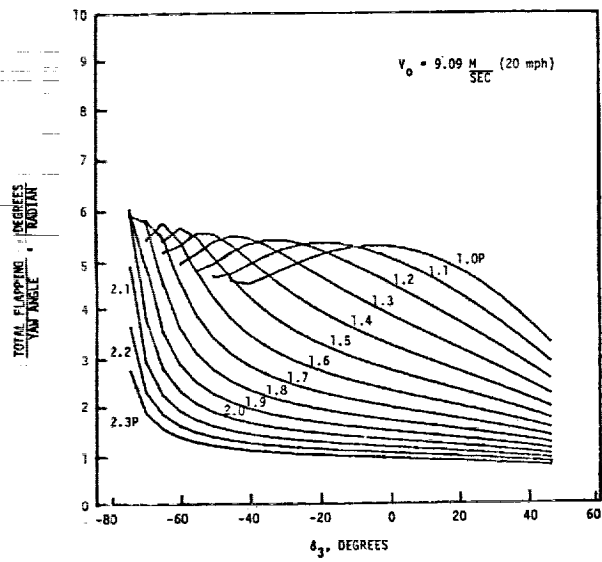


Figure 3 - Total flapping due to yaw angle versus δ_3 for fourteen normal frequencies.

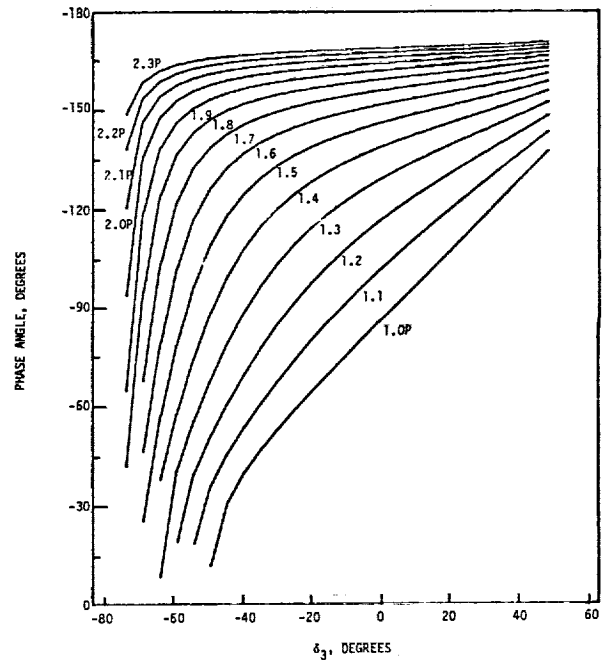


Figure 5 - Phase of flapping response to yaw position vs δ_3 for fourteen normal frequencies.

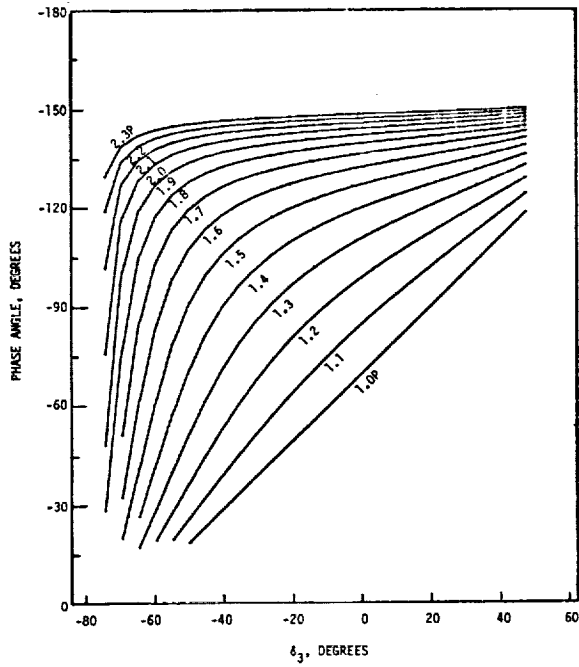


Figure 6 - Phase of flapping response to yaw rate vs δ_3 for fourteen normal frequencies.

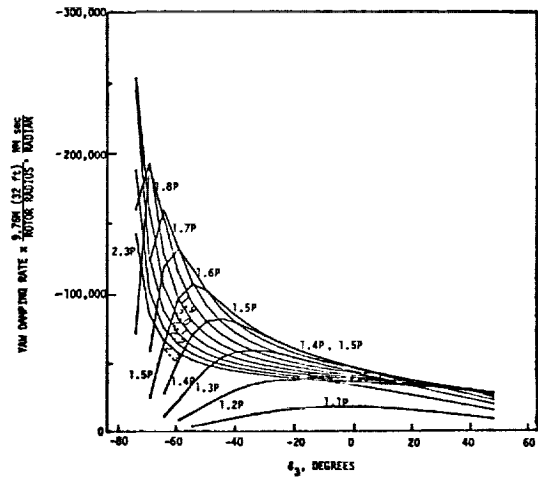


Figure 8 - Yaw damping rate vs δ_3 for thirteen normal frequencies.

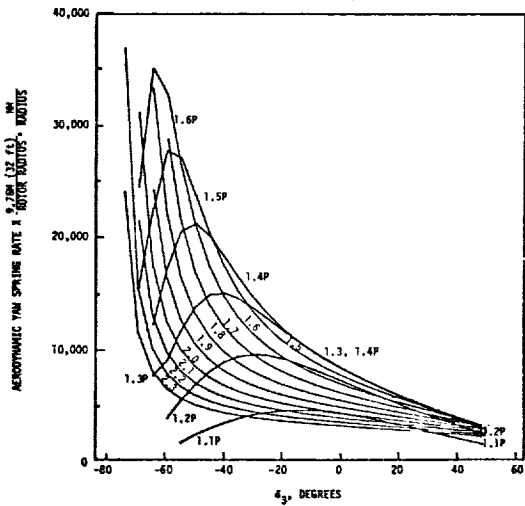


Figure 7 - Aerodynamic spring rate vs δ_3 for thirteen normal frequencies.

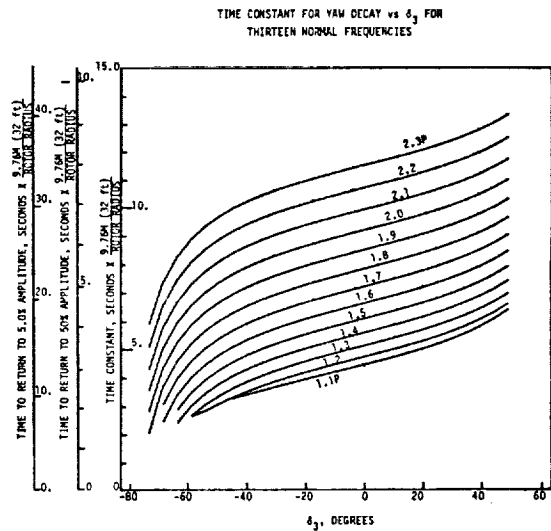


Figure 9 - Time constant for yaw decay vs δ_3 for thirteen normal frequencies.

QUESTIONS AND ANSWERS

F.W. Perkins

From: J. Cochem

Q: Can you physically explain the significance of $1.4 P$, and its effect on yaw dynamics?

A: $1.4 P$ is just that normal frequency which maximizes the product of K_β and β_{15} which gives the yaw moment. Increasing K_β , consequently the normal frequency, decreases β_{15} more rapidly than K_β increases.

SECOND DOE/NASA WIND TURBINE DYNAMICS WORKSHOP

Electrical & Control Systems

Session Chairman - L.J. Gilbert (NASA LeRC)

"VAWT Drive Train Transient Dynamics"
D.B. Clauss
(Sandia Labs.)

"Dynamics & Stability of WTG's"
E.N. Hinrichsen
P.J. Nolan
(Power Tech., Inc.)

"Kaman 40 kW WTG - Control System Dynamics"
R. Perley
(Kaman Aerospace Corp.)

"Automatic Control Algorithm Effects on Energy Production"
G. McNerney
(U. of New Mexico)

"Effect of Wind Power Changes on Utility System Dispatch"
R.A. Schlueter
G.L. Park
(Michigan State Univ.)

